

A microRNA program regulates the balance between cardiomyocyte hyperplasia and hypertrophy and stimulates cardiac regeneration

¹ Andrea Raso; ¹ Ellen Dirkx; ^{1,2} Vasco Sampaio-Pinto; ^{1,3} Hamid el Azzouzi; ^{4,5} Ryan J. Cubero; ⁶ Daniel W. Sorensen; ¹ Lara Ottaviani; ¹ Servé Olieslagers; ⁷ Manon M. Huibers; ⁷ Roel de Weger; ⁸ Sailay Siddiqi; ⁹ Silvia Moimas; ⁹ Consuelo Torrini; ⁹ Lorena Zentillin; ⁹ Luca Braga; ² Diana S. Nascimento; ^{1,10} Paula A. da Costa Martins; ⁶ Jop H. van Berlo; ⁸ Serena Zacchigna; ^{9,11} Mauro Giacca and ¹ Leon J. De Windt*

¹*Department of Molecular Genetics, Faculty of Science and Engineering, Faculty of Health, Medicine and Life Sciences, Maastricht University, 6229 ER Maastricht, The Netherlands;*

²*i3S - Instituto de Investigação e Inovação em Saúde, INEB - Instituto Nacional de Engenharia Biomédica, ICBAS - Instituto de Ciências Biomédicas de Abel Salazar, University of Porto, Porto, Portugal.*

³*Department of Molecular Genetics, Erasmus University MC, 3015 GD Rotterdam, The Netherlands;*

⁴*The Abdus Salam International Centre for Theoretical Physics, 34151 Trieste, Italy;*

⁵*IST Austria, 3400 Klosterneuburg, Austria;*

⁶*Stem Cell Institute and Lillehei Heart Institute, Department of Medicine, University of Minnesota, Minneapolis, U.S.A.*

⁷*Department of Pathology, University Medical Center Utrecht, 3584 CX Utrecht, The Netherlands;*

⁸*Department of Cardiothoracic Surgery, Radboud University Medical Center, Nijmegen, the Netherlands;*

⁹*International Centre for Genetic Engineering and Biotechnology (ICGEB), Trieste, Italy;*

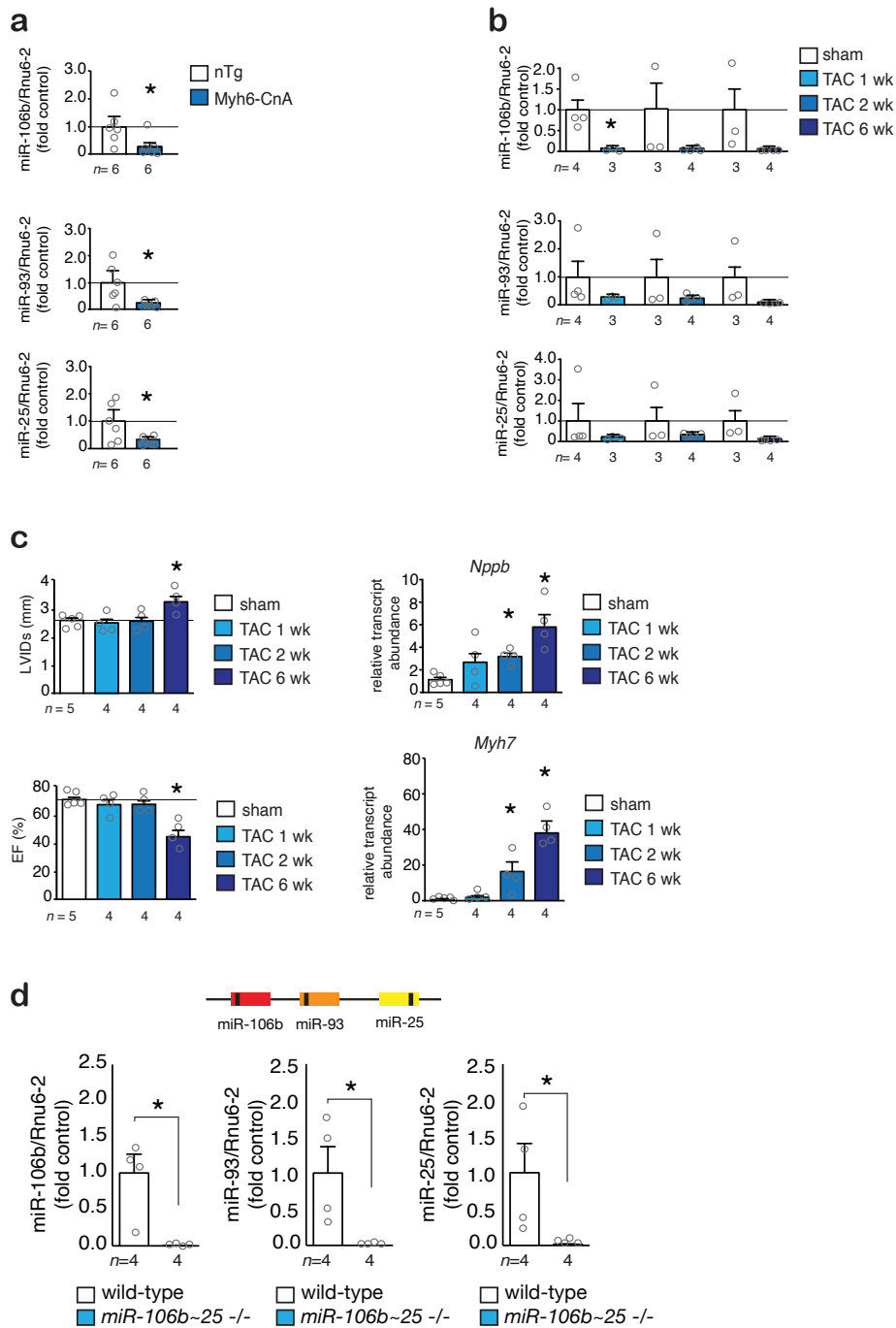
¹⁰*Department of Physiology and Cardiothoracic Surgery, Faculty of Medicine, University of Porto, Porto, Portugal.*

¹¹*School of Cardiovascular Medicine and Sciences, King's College London, London, UK.*

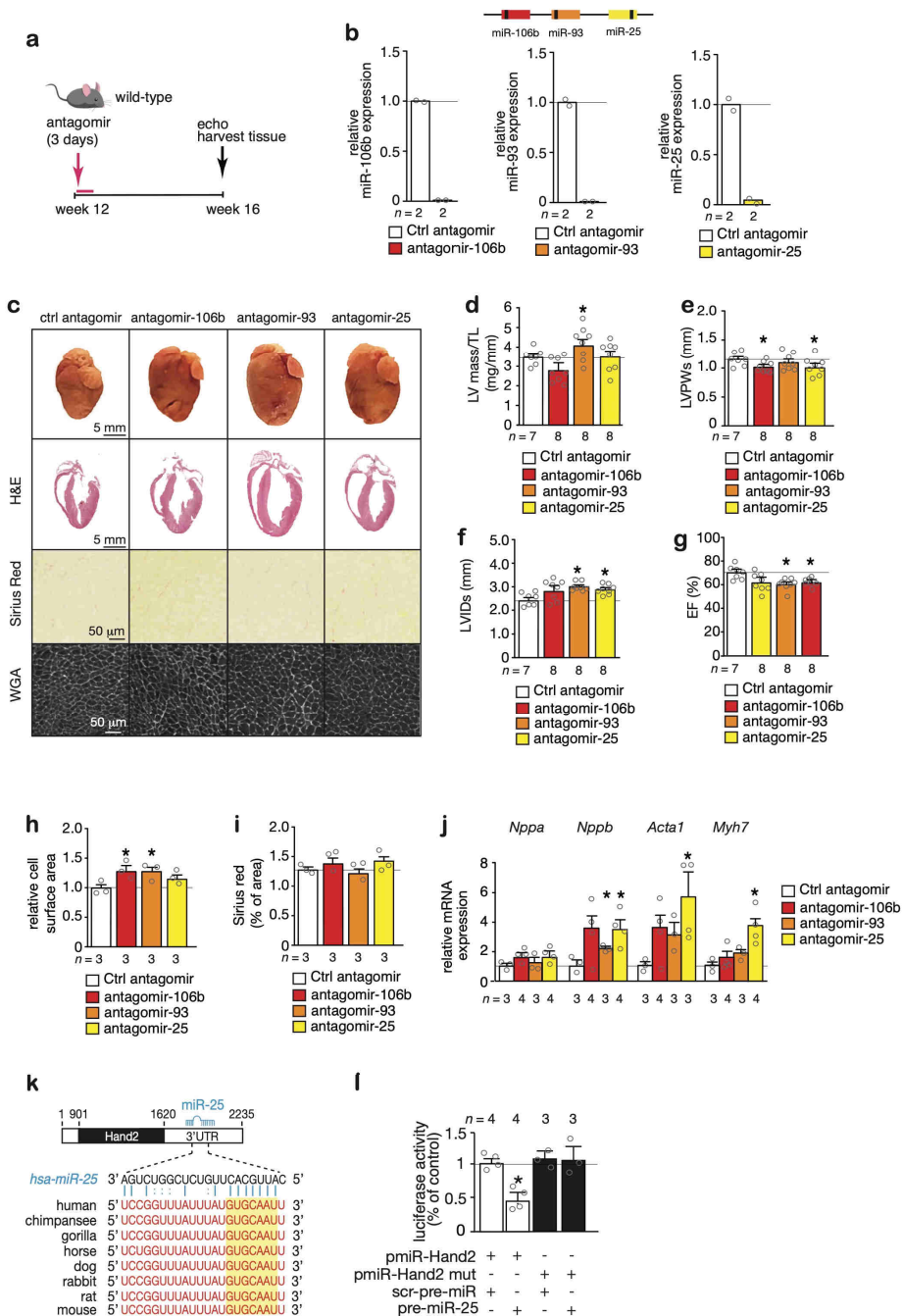
A.R. and E.D. contributed equally to this work

Supplementary Figures 1-6
Supplementary Table 1

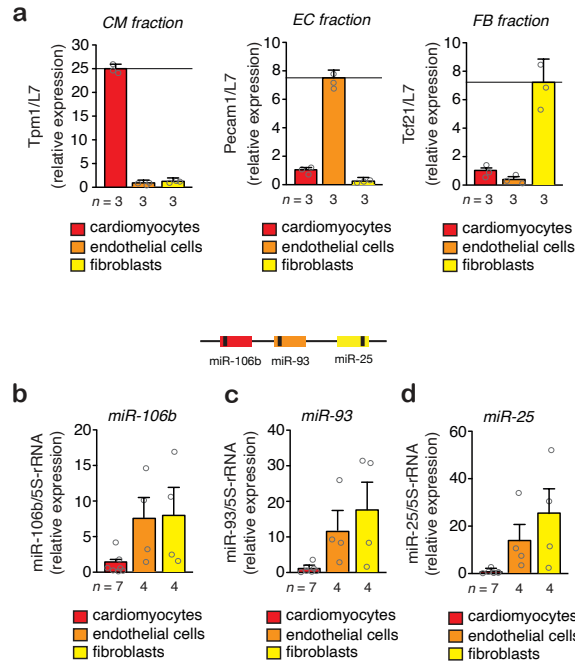
Supplementary Figures



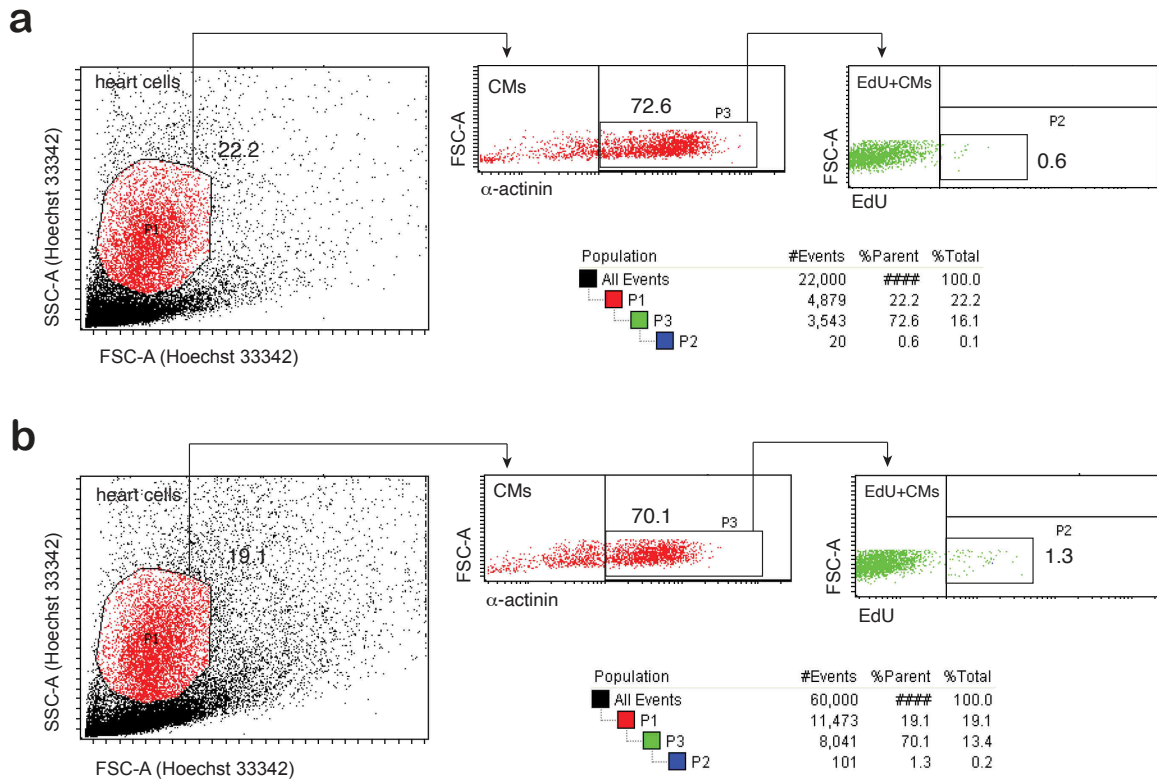
Supplementary Figure 1 | *miR-106b~25* cluster expression. (a) Real-time PCR analysis of *miR-106b*, *miR-93* and *miR-25* abundance in hearts from non-transgenic (nTg) or Myh6-CnA transgenic mice or in (b) mice subjected to transverse aortic constriction (TAC) for 1, 2 or 6 weeks. (c) Indices of cardiac dilation (LVIDs), function (EF) and expression of *Nppb* and *Myh7* in mice subjected to TAC for 1, 2 or 6 weeks. (d) Real-time PCR analysis of *miR-106b*, *miR-93* and *miR-25* abundance in hearts of wild-type (WT) or *miR-106b~25* null mice, *n* refers to the number of hearts. **P* < 0.05 vs corresponding control group (error bars are s.e.m.). Statistical analysis consisted of a two-tailed Student's t-test. Source data are provided as a Source Data file.



Supplementary Figure 2 | *miR-106b~25* silencing with single antagomirs. (a) Workflow of the study. **(b)** Real-time PCR analysis of *miR-106b*, *miR-93* and *miR-25* expression in hearts from mice receiving control (ctrl) antagomir or antagomir against a specific miRNA. **(c)** Representative images of whole hearts (top panels), H&E-stained sections (second panel), Sirius Red stained sections (third panel) and WGA-stained (fourth panel) histological sections. Quantification of **(d)** LV/BW ratio, **(e)** LVPWs, **(f)** LVIDs, and **(g)** EF of mice that received indicated antagomirs. Quantification of **(h)** cell surface areas by WGA-staining and **(i)** fibrotic area by Sirius Red staining. **(j)** Real-time PCR analysis of *Nppa*, *Nppb*, *Acta1*, and *Myh7*; *n* refers to number of hearts. **(k)** Location and evolutionary conservation of hsa-miR-25 seed region on *Hand2*. **(l)** Activity assay of luciferase reporter constructs shows the binding of hsa-miR-25 to the 3'UTR of *Hand2*, *n* refers to number of transfection experiments. **P* < 0.05 vs corresponding control group (error bars are s.e.m.). Statistical analysis consisted of a two-tailed Student's t-test **(l)** or a One-way ANOVA followed by Dunnett multiple comparison test **(d-g)**. Source data are provided as a Source Data file.

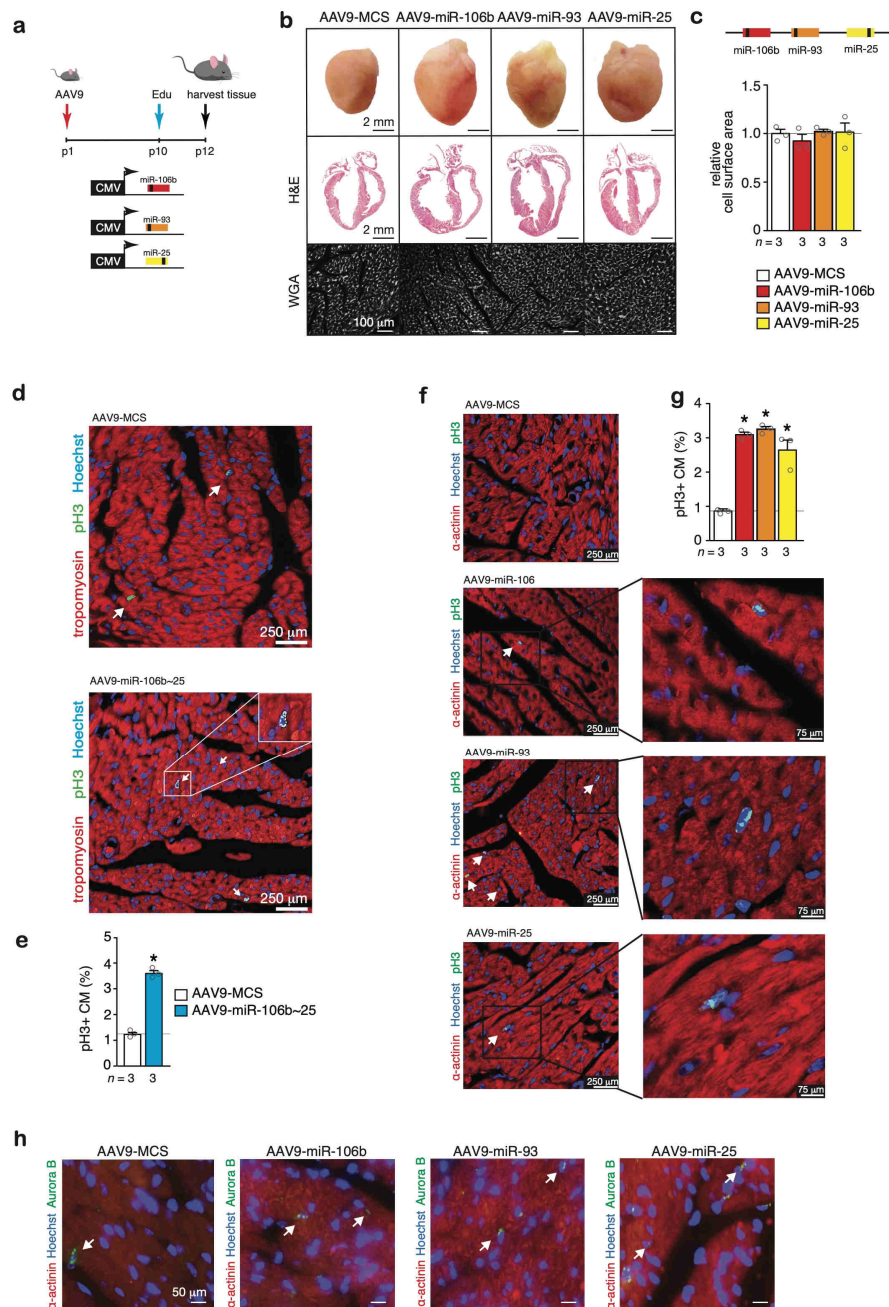


Supplementary Figure 3 | *miR-106b~25* cluster expression in adult mouse heart cells. (a) Real-time PCR analysis of marker genes for Tropomyosin 1 (Tpm1), Platelet endothelial cell adhesion molecule (Pecam1) and Transcription factor 21 (Tcf21) in cardiomyocytes (CMs), endothelial cells (ECs) and fibroblasts (FBs) following enzymatic dissociation of adult mouse hearts followed by column-based magnetic cell isolation. Real-time PCR analysis of *miR-106b*, *miR-93* and *miR-25* abundance in **(b)** CMs, **(c)** ECs or **(d)** FBs, *n* refers to the number of hearts (error bars are s.e.m.). Source data are provided as a Source Data file.

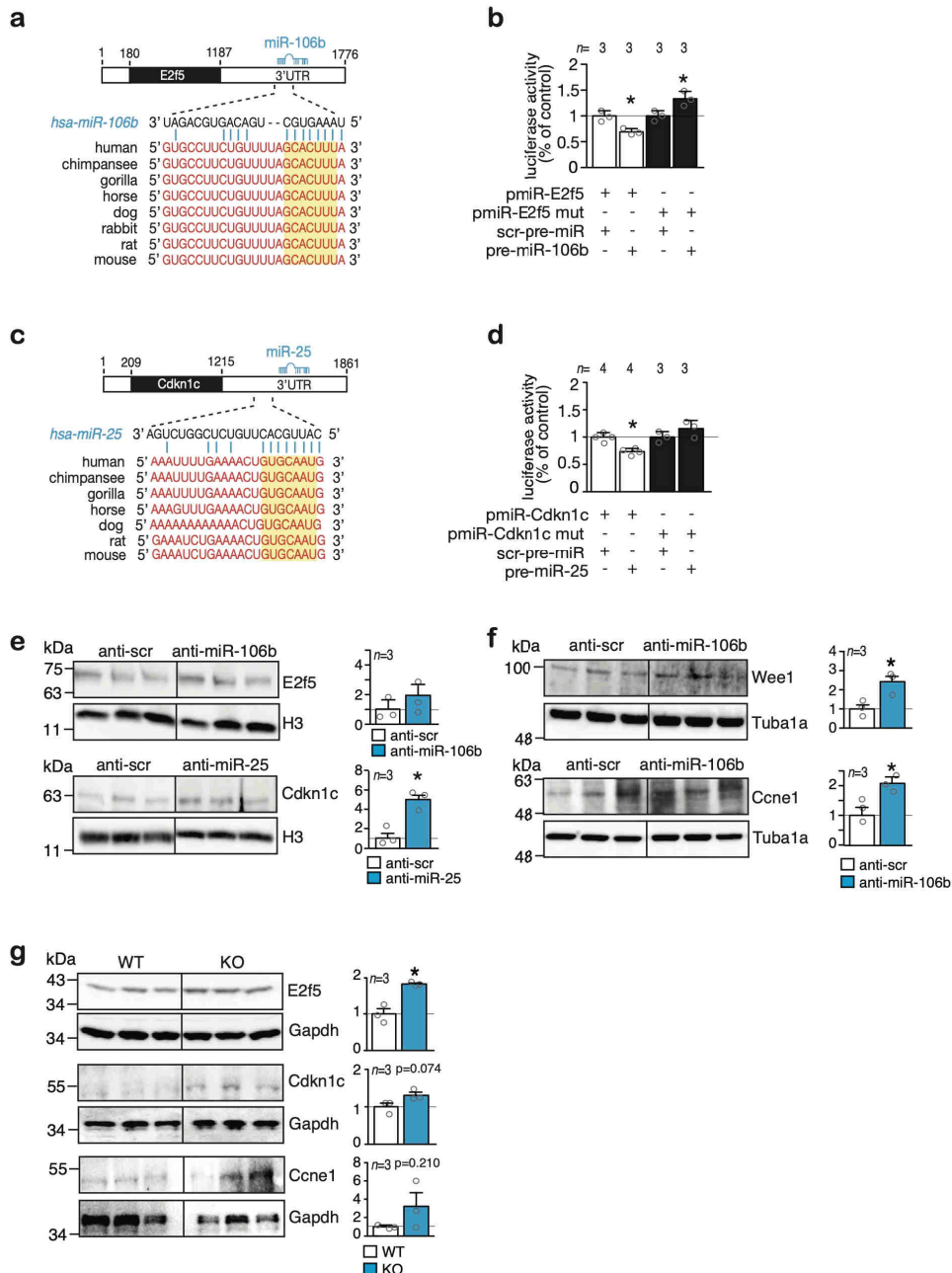


Supplementary Figure 4 | Overexpression of *miR-106b~25* stimulates CM proliferation.

Neonatal mice at age p1 received AAV9-MCS or AAV9-miR106b~25, at p10 administered a single EdU injection and 2 days later cardiomyocytes (CMs) from $n=5$ hearts in each condition were isolated, pooled and analyzed by flow cytometry. **(a)** Gating strategy for the detection of EdU+CMs within myocardial cells from mice that received AAV9-MCS. **(b)** Gating strategy for the detection of EdU+CMs within myocardial cells from mice that received AAV9-miR106b~25.



Supplementary Figure 5 | Overexpression of *miR-106b*, *miR-93* or *miR-25* induces cardiac enlargement by stimulating cardiomyocyte proliferation. (a) Design of the study. **(b)** Representative images of whole hearts (top panels), H&E-stained histological sections of four-chamber view (second panel) and WGA-stained (third panel) histological sections. **(c)** Quantification of cell surface areas. **(d)** Representative confocal microscopy images and **(e)** quantification of pH3 positive cardiomyocytes (CMs; α -actinin+, pH3+) in heart sections of mice receiving AAV9-MCS or AAV9-miR-106b~25 and stained for tropomyosin, pH3 and Hoechst. **(f)** Representative confocal microscopy images and **(g)** quantification of the number of pH3 positive CMs (α -actinin+, pH3+) in heart sections of mice receiving AAV9-MCS, AAV9-miR-106b, AAV9-miR-93 or AAV9-miR-25 and stained for α -actinin, pH3 and Hoechst, *n* refers to number of hearts. **(h)** Representative confocal microscopy images of heart sections of mice receiving AAV9-MCS, AAV9-miR-106b, AAV9-miR-93 or AAV9-miR-25 and stained for α -actinin, Aurora B and Hoechst. **P* < 0.05 vs corresponding control group (error bars are s.e.m.). Statistical analysis consisted of a two-tailed Student's t-test **(e)** or a One-way ANOVA followed by Dunnett multiple comparison test **(c,g)**. Source data are provided as a Source Data file.



Supplementary Figure 6 | *miR-106b~25* targetome validation. (a) Location and evolutionary conservation of the *hsa-miR-106b* seed region on *E2f5*. **(b)** Activity assay of luciferase reporter constructs shows the binding of *hsa-miR-106b* to the 3'UTR of *E2f5*. **(c)** Location and evolutionary conservation of the *hsa-miR-25* seed region on *Cdkn1c*. **(d)** Activity assay of luciferase reporter constructs shows the binding of *hsa-miR-25* to the 3'UTR of *Cdkn1c*, *n* refers to number of transfection experiments. **(e)** Western blot analysis of endogenous *E2f5* and *Cdkn1c* and histone 3 (H3) as a loading control in cardiomyocytes transfected with a control anti-miR, or anti-miRs for *miR-106b* or *miR-25*. **(f)** Western blot analysis of endogenous *Wee1*, *Ccne1* and Tubulin-a (*Tuba1a*) as a loading control in cardiomyocytes transfected with a control anti-miR, or an anti-miR for *miR-106b*. **(g)** Western blot analysis of endogenous *E2f5*, *Cdkn1c*, *Ccne1* and *Gapdh* as a loading control in hearts from WT versus *miR-106b~25* KO mice, *n* refers to the number of animals. * $P < 0.05$ vs corresponding control group (error bars are s.e.m.). Statistical analysis consisted of a two-tailed Student's t-test. Source data are provided as a Source Data file.

Supplementary Table 1. real-time PCR primers used in the study

Gene name	Gene identification		sequence
<i>Nppa</i>	NM_008725	FW	TCTTCCTCGTCTTGGCCTTT
		RV	CCAGGTGGTCTAGCAGGTTT
<i>Nppb</i>	NM_008726	FW	TGGGAGGTCCTCTATCCT
		RV	GGCCATTCCTCCGACTTT
<i>Acta1</i>	NM_009606	FW	CCGGGAGAAGATGACTCAA
		RV	GTAGTACGGCC GGAAGCATA
<i>Myh7</i>	NM_080728	FW	CGGACCTTGAAGACCAGAT
		RV	GACAGC TCCCATTCTCTGT
<i>Tpm1</i>	NM_001164256	FW	GTATGAAGAGGTGGCCCGTA
		RV	CGAGTTTCAGCCTCCTTCAG
<i>Pecam1</i>	NM_001032378	FW	AACAGAGCTGTTTCCAAGC
		RV	GTGAAGTTGGCTACAGGTGT
<i>Tcf21</i>	NM_011545	FW	CTTCTCCAGGCTCAAGACCA
		RV	ATAAAGGGCCACGTCAGGTT
<i>Rpl7</i>	NM_011291	FW	GAAGCTCATCTATGAGAAGGC
		RV	AAGACGAAGGAGCTGCAGAAC

All oligos are depicted in 5' --> 3' direction. FW, forward; RV, reverse.